agronomy

MDPI

Article

Remote Sensing Meets Agronomy: A Three-Year Field Study of Tritordeum's Response to Enhanced Efficiency Fertilisers

George Papadopoulos [1,2,*], Ioannis Zafeiriou [3], Evgenia Georgiou [3], Antonia Oikonomou [4], Antonios Mavroeidis [1], Panteleimon Stavropoulos [1], Ioanna Kakabouki [1], Spyros Fountas [2] and Dimitrios Bilalis [1]

[1] Laboratory of Agronomy, Department of Crop Science, Agricultural University of Athens, 11855 Athens, Greece; antoniosmauroeidis@gmail.com (A.M.); stavropoulosp@aua.gr (P.S.); i.kakabouki@aua.gr (I.K.); bilalis@aua.gr (D.B.)
[2] Laboratory of Agricultural Engineering, Department of Natural Resources Management & Agricultural Engineering, School of Environment and Agricultural Engineering, Agricultural University of Athens, 11855 Athens, Greece; sfountas@aua.gr
[3] Laboratory of Soil Science and Agricultural Chemistry, Agricultural University of Athens, 11855 Athens, Greece; ioannis.zafeiriou@aua.gr (I.Z.); georgiounina18@gmail.com (E.G.)
[4] Laboratory of Minerology and Geology, Department of Natural Resources and Agricultural Engineering, School of Environment and Agricultural Engineering, Agricultural University of Athens, 75 Iera Odos Str., Votanikos, 11855 Athens, Greece; ninaoik2001@gmail.com
* Correspondence: gpapadopoulos@aua.gr

Abstract

This three-year field study evaluated the agronomic and physiological responses of Tritordeum to nitrogen fertilisation strategies under Mediterranean conditions using an integrated approach combining GDD-aligned phenological monitoring, UAV-based multispectral imaging, and soil analysis. Treatments included conventional urea, urea with a nitrification inhibitor (U+NI; DMPP-based), and urea with a urease inhibitor (U+UI; NBPT-based), compared to an unfertilised control. All nitrogen treatments significantly increased grain yield, reaching up to 2319 kg ha^{-1} under the nitrification inhibitor treatment (26% higher than the control), and protein content, which peaked at 16.04% under urea. Temporal analysis revealed that urea with nitrification inhibitors consistently enhanced plant height, canopy greenness, and pigment retention during flowering to ripening stages, with NDVI and MCARI peaking under U+NI in 2025. In contrast, urea with urease inhibitor promoted greater early-season biomass and height. Soil nitrogen retention was slightly improved under both EEF treatments, with no adverse effects on pH or salinity. The strong alignment between UAV-derived indices and agronomic traits supports their use for monitoring nitrogen response. These findings demonstrate the benefits of a stage-specific fertilisation strategy, deploying urea with nitrification inhibitor early and urea with urease inhibitor during peak vegetative growth, to improve nitrogen synchrony with crop demand and support sustainable crop management in Tritordeum.

Keywords: multispectral vegetation indices; UAV; enhanced efficiency fertilizers; urease inhibitor; nitrification inhibitor; tritordeum; Mediterranean agroecosystems

Academic Editor: Xiongkui He

Received: 10 August 2025
Revised: 11 September 2025
Accepted: 18 September 2025
Published: 22 September 2025

Citation: Papadopoulos, G.; Zafeiriou, I.; Georgiou, E.; Oikonomou, A.; Mavroeidis, A.; Stavropoulos, P.; Kakabouki, I.; Fountas, S.; Bilalis, D. Remote Sensing Meets Agronomy: A Three-Year Field Study of Tritordeum's Response to Enhanced Efficiency Fertilisers. *Agronomy* **2025**, *15*, 2244. https://doi.org/10.3390/agronomy15092244

1. Introduction

In recent years, smart farming technologies have revolutionized crop monitoring, enabling rapid, non-invasive, and cost-effective assessment of growth, health, and nutritional status. Multispectral vegetation indices (VIs) derived from remote sensing platforms, such

as unmanned aerial vehicles (UAVs) and satellites, have emerged as powerful tools for tracking key agronomic traits, including biomass accumulation, plant height, and overall crop vigor [1–5]. Several VIs, notably the Normalized Difference Vegetation Index (NDVI), Green NDVI (GNDVI), Normalized Difference Red Edge Index (NDRE), and Modified Chlorophyll Absorption Ratio Index (MCARI), are widely used due to their sensitivity to chlorophyll content, canopy structure, and photosynthetic activity [6–9]. Given N's critical role in chlorophyll synthesis, enzyme activation, and overall plant growth, these indices provide indirect yet reliable indicators of crop N status [10].

NDVI, commonly used to estimate canopy greenness, frequently correlates with N content, especially in cereals [9], however NDVI often saturates under dense canopies. GNDVI and NDRE mitigate this limitation by utilizing the green and red-edge spectral bands, respectively, improving N detection across growth stages [6,8,11]. MCARI further enhances sensitivity by focusing on chlorophyll absorption while minimizing canopy structure effects [7]. Multispectral imaging has consistently proven effective for assessing N status in cereals; for example, Bagheri, (2017) [12] reported high correlation between multispectral data and canopy N status in maize, while other studies have demonstrated its usefulness for detecting nitrogen stress in winter wheat [13].

While multispectral VIs timely and spatially rich insights into crop status, their interpretation becomes more robust when complemented by foundational agronomic parameters, especially in the context of N application assessment. Traits such as plant height, fresh and dry biomass, spike length, thousand grain weight (TGW), and seed protein content are well-established indicators of plant growth, nutrient uptake, and yield potential [14,15]. These parameters have long served as reliable proxies for crop vigor and are critical for evaluating physiological responses to fertilisation regimes under varying environmental conditions. Equally important is the timing of data collection, as crop development and N demand vary significantly across growth stages. Standardizing phenological monitoring using Growing Degree Days (GDDs), a thermal time index that integrates daily temperature, has emerged as a reliable method for capturing crop development in a temperature-driven and climate-resilient manner [16]. This is particularly relevant in Mediterranean systems, where climate variability, including heatwaves and irregular rainfall, often disrupts calendar-based staging [17]. By aligning agronomic measurements and remote sensing data with GDD-calibrated phenological stages, a more precise understanding of crop responses to N fertilisation can be achieved, enhancing the comparability and reliability of treatment effects across seasons and conditions.

Tritordeum (×Tritordeum Ascherson et Graebner) is an emerging amphiploid cereal developed through the hybridization of durum wheat (Triticum turgidum) and wild barley (Hordeum chilense), recognized for its adaptability to Mediterranean agro-climatic conditions and potential to support climate-resilient, low-input farming systems [16,18,19]. Its notable agronomic traits, such as tolerance to drought and heat stress, moderate to high protein content, and suitability for organic farming, make it a valuable alternative to traditional cereals like wheat and barley, particularly in countries such as Greece, Spain, and Italy [20,21]. Despite these promising characteristics, the crop's response to N fertilisation remains largely underexplored, with only limited insights available compared to its wheat and barley parents [22]. At the same time, Enhanced Efficiency Fertilisers (EEFs), including urease inhibitors such as N-(n-butyl) thiophosphoric triamide (NBPT) and nitrification inhibitors like dicyandiamide (DCD) and nitrapyrin, have shown significant potential to reduce N losses and enhance nitrogen use efficiency (NUE) in major cereals such as wheat and maize [23–27]. For instance, NBPT has been shown to reduce ammonia volatilisation by over 50% and improve grain yield under high-temperature conditions [27], while DCD and nitrapyrin have effectively lowered nitrate leaching and nitrous oxide emissions in

intensive cropping systems [28,29]. However, limited studies have examined how Tritordeum performs under EEF regimes over multiple growing seasons using an integrated remote sensing and agronomic approach. Given its increasing relevance for Mediterranean cereal production, understanding Tritordeum's physiological and agronomic responses to EEFs is essential to design fertilization strategies that optimize yield and grain quality while mitigating environmental impacts.

This study aims to address the current research gap by conducting a three-year field experiment to evaluate Tritordeum's response to N application under EEFs, combining remote sensing, agronomic measurements, and soil fertility analysis. Three fertilisation strategies were assessed: conventional urea, urea combined with a urease inhibitor (NBPT), urea combined with a nitrification inhibitor (DMPP), and an unfertilised control. Key agronomic traits and UAV-derived multispectral VIs were monitored at five phenological stages, standardized using GDDs to ensure temporal consistency. Additionally, baseline and post-harvest soil analyses were conducted to assess potential long-term effects of EEFs on soil fertility. This integrated, multi-year approach provides novel insights into Tritordeum's physiological and agronomic response to N fertilisation strategies, offering a basis for tailored, sustainable fertilizer management in Mediterranean cereal systems.

2. Materials and Methods

2.1. Experimental Site and Design

A three-year field experiment was carried out in Greece from November 2022 to May 2025 at the experimental site of the Laboratory of Agronomy, Agricultural University of Athens (37°59′01.83″ N, 23°42′07.37″ E; altitude: 30 m). The geographical location of the experimental field is shown in Figure 1. The plant material used was 'Bulel', the second commercial cultivar of Tritordeum (×Tritordeum martinii A. Pujadas, nothosp. nov.), which was registered in 2013 with the Community Plant Variety Office (CPVO). To underline the previous management history of the experimental site, it was cultivated with wheat and barley. Climatic data, including mean air temperature and total precipitation, for the three years, were obtained from the National Observatory of Athens ("Athens-Votanikos/Gazi Region" weather station—"Link: http://meteo.gr/stations/athens/" (accessed on 20 June 2025)). The data are presented in detail in Figure 2.

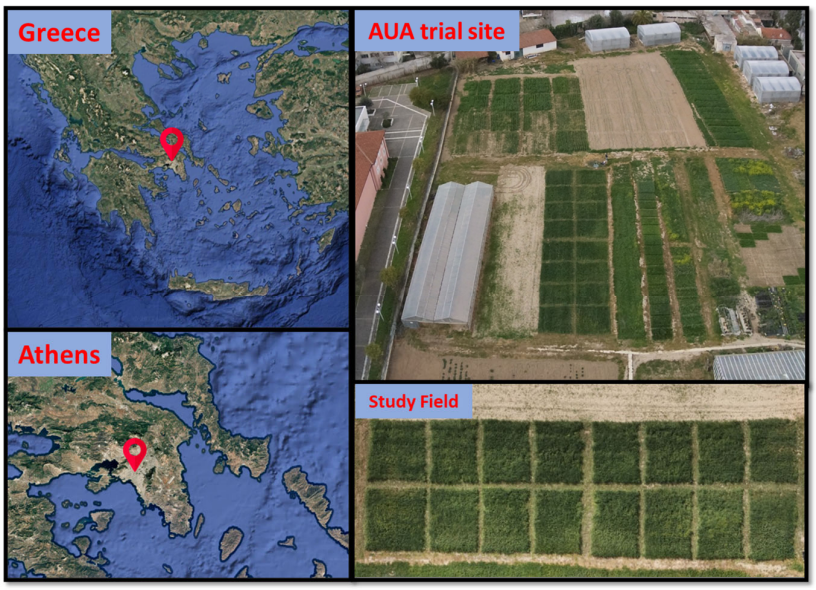

Figure 1. Geographical location of the experimental field within Greece.

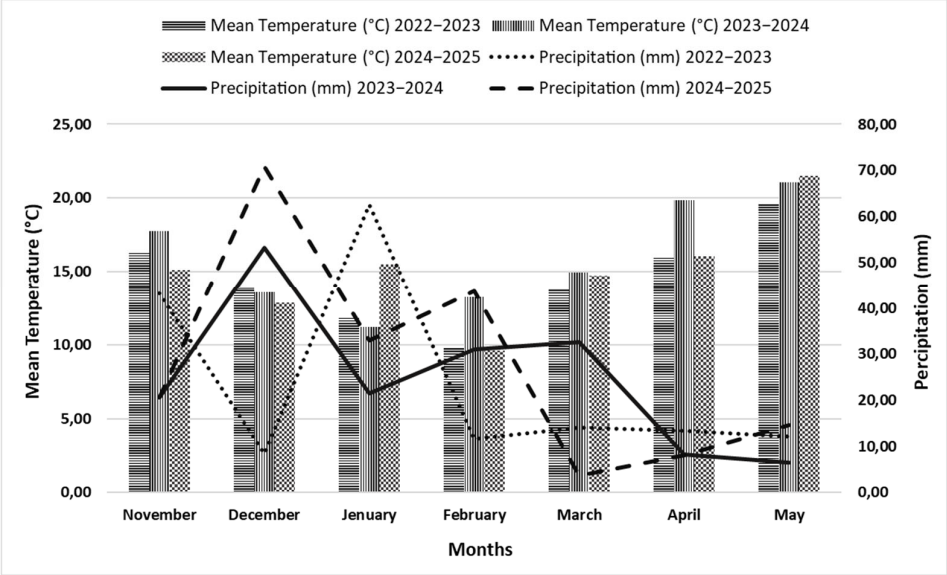

Figure 2. Climatic Data over the cultivation seasons, throughout the duration of the experiment.

A completely randomized block design (CRBD) was employed, incorporating three urea-based fertilization treatments, each replicated four times. The CRBD was applied at the beginning of the trial (2022–2023), and the same plots consistently received the same fertilisation treatments across all three cropping seasons, ensuring treatment continuity and allowing assessment of cumulative effects. Statistical analyses were performed separately for each year to account for interannual variability. The layout of the experimental design is illustrated in Figure 3. An unfertilized plot served as the control treatment (C). The three urea-based fertilisation treatments were as follows: (U) urea (46-0-0), (U+NI) urea (46-0-0) with a nitrification inhibitor [3,4-dimethyl-1H-pyrazole phosphate (DMPP; 0.276%)] and (U+UI) urea (46-0-0) with a urease inhibitor [NBPT(N-(n-butyl) thiophosphoric triamide) 0.06%]. The experimental field covered an area of 420 m^2, with each plot measuring 4.0 m × 5.0 m (20 m^2).

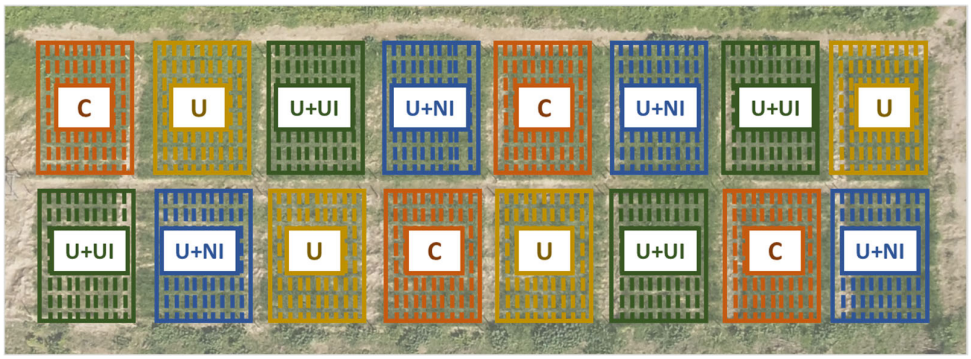

Figure 3. Layout of the experimental design.

Seeds were sown at a depth of 2–3 cm, with 20 cm row spacing with the seeding density estimated at approximately 2.5 million seeds ha^{-1}. Fertilizer treatments were applied in two stages: a basic application (115 kg N ha^{-1}) and second application (60 kg N ha^{-1}) 40 days after sowing. Both applications followed the assigned treatments (U, U+NI, U+UI). Weed control was performed weekly by hand, and at maturity, the entire plot was manually harvested. Figure 4 provides a detailed schedule of field operations during the three-year experimental period.

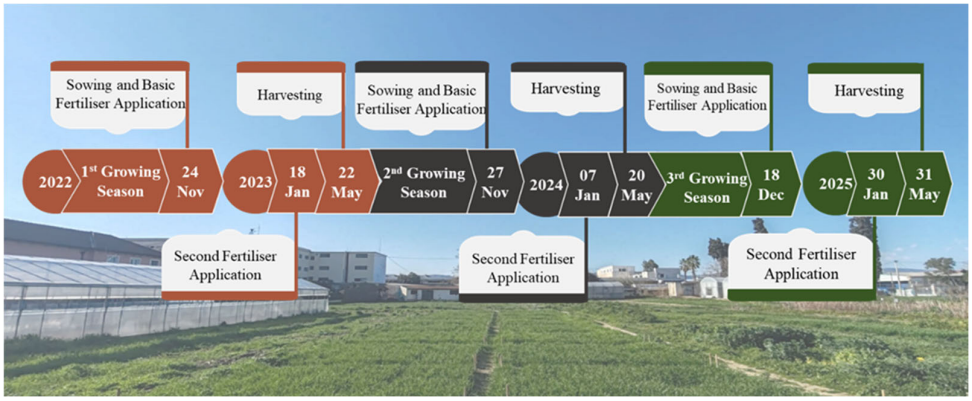

Figure 4. Detailed schedule of field operations during the experimental period (2022–2025).

2.2. Measured Parameters

2.2.1. Soil Sampling and Analysis

Soil sampling was conducted twice during the experimental period: initially, before the first cultivation season (November 2022), to assess baseline soil properties, and subsequently at the end of the final season (May 2025), to evaluate the cumulative effect of the different fertilization strategies. In both phases, topsoil samples (0–20 cm) were collected from the experimental field, placed in sterile plastic bags, and transported to the laboratory. Samples were air-dried, passed through a 2 mm sieve, and stored for further analysis. Soil texture was determined only at the first phase of sampling using the Bouyoucos hydrometer method [30]. Soil organic matter (SOM) content was analyzed using the Walkley–Black dichromate oxidation method, while soil pH and electrical conductivity (EC) were measured electrometrically in a 1:1 (w/v) soil-to-water suspension using an automated pH meter and conductivity meter (Selecta 2000, J.P. Selecta S.A., Barcelona, Spain) [31,32]. Available phosphorus was determined by the Olsen method [33], and total N concentration was measured using the Kjeldahl method [34]. Exchangeable cations were extracted with 1 M ammonium acetate following the method of Thomas, 1982 [35]. Micronutrient concentrations, including copper (Cu), manganese (Mn), iron (Fe), and zinc (Zn), were determined using the DTPA extraction method in a 1:2 (w/v) soil-to-ammonium acetate suspension [36].

2.2.2. Phenological Staging Based on Growing Degree Days

GDDs were calculated to determine the critical phenological stages of Tritordeum during each growing season. GDDs enable consistent comparison of crop development across the three experimental years. Specifically, daily GDDs were calculated using the following Equation (1), as described by [37].

$$GDDs = \frac{(Tmin + Tmax)}{2} - Tb \quad (1)$$

where $Tmax$ and $Tmin$ are the maximum and minimum daily air temperature (°C), and Tb is the base temperature for the crop. Based on literature values for durum wheat (Triticum turgidum) and wild barley (Hordeum vulgare), Tb was set at 5.0 °C [16]. Phenological stages were identified in the field according to the BBCH scale [38], and the corresponding accumulated GDDs were recorded at each observed stage. These phenological stages were used to coordinate agronomic sampling and conduct stage-specific measurements.

2.2.3. Agronomic Traits and Qualitative Characteristics

Agronomic measurements were conducted at five key phenological stages, stem elongation, flowering, seed filling, and ripening/senescence, determined each season based on

accumulated GDDs. At each stage, five representative plants were randomly sampled from each plot and transported to the laboratory, where plant height and fresh weight were measured. At the final phenological stage (ripening/senescence), spike length was measured to assess any morphological differences influenced by the fertilization treatments. The overall yield was calculated by harvesting the entire plot, with seed extraction performed using a Wintersteiger LD350 (Wintersteger, Ried im Innkreis, Austria) plot combine harvester. After harvesting the Thousand grain weight (TGW) was determined by randomly selecting and weighing 1000 seeds from each plot. For the protein analysis, seeds were oven-dried at 60 °C using a drying oven (DHG-9203A, Zhengzhou Wollen, China)until a constant weight was achieved. The dried samples were then ground to a particle size of less than 0.5 mm using a stainless-steel mill. Total N concentration in seeds was determined using the Kjeldahl method, following the procedure described by Nelson and Sommers (1980) [39], and protein content was calculated as N% × 5.7 [40].

2.2.4. Multispectral Indices—UAV Flights

Remote sensing measurements were conducted using a DJI Phantom 4 Multispectral UAV (DJI, Shenzhen, China) (Figure 5), equipped with an integrated multispectral camera comprising five monochrome sensors (blue: 450 ± 16 nm, green: 560 ± 16 nm, red: 650 ± 16 nm, red edge: 730 ± 16 nm, near-infrared: 840 ± 26 nm) and one RGB sensor for visible light imaging. This system enables high-resolution, co-registered imagery for vegetation index calculation. Flights were conducted at 20 m height, with a GSD of 1.1 cm pixel^{-1}, and 80% overlap and 80% sidelap between images. The camera captured one image every 2.0 s, acquiring six simultaneous spectral images of each location from the same viewing angle. All UAV flights were conducted between late morning and midday to ensure consistent, near-vertical solar illumination and minimize shadow interference. Image acquisition was performed at five key phenological stages, aligned with agronomic trait measurements. The collected multispectral images were processed using PIX4Dfields (v2.9.5) to generate high-resolution orthomosaics via photogrammetric reconstruction. Subsequently, four VIs, NDVI, GNDVI, NDRE, and MCARI, were calculated within the same software environment using the formulas presented in Table 1.

Figure 5. DJI Phantom 4 Multispectral UAV used for remote sensing measurements.

The selection of these indices was primarily based on their extensive utilization in the evaluation of vegetation vigor, chlorophyll content, and canopy structure. Each index employs a distinct region of the electromagnetic spectrum, such as the visible, red-edge, and near-infrared, thereby providing complementary insights into health and biomass of plants. The resulting orthomosaics and index layers were projected at WGS 84/UTM zone 34N coordinate system, and imported into ArcGIS (v10.8.1, ESRI) environment, for geostatistical analyses at plot level. This workflow ensured accurate spatial alignment and allowed for detailed

study of spatial variability among treatments. Spatial analysis was based on the extraction of vegetation index values from systematically sampled locations within each plot, ensuring unbiased representation of canopy variability for subsequent statistical evaluation.

Table 1. Multispectral Vegetation Indices used in the study and their mathematical formulations.

Multispectral Indices	Equation	Reference
NDVI	$\frac{(NIR-RED)}{(NIR+RED)}$	[41] (Rouse & Haas, 1974)
GNDVI	$\frac{(NIR-Green)}{(NIR+Green)}$	[42] (Gitelson et al., 2005)
NDRE	$\frac{(NIR-RedEdge)}{(NIR+RedEdge)}$	[6] (Barnes et al., 1999)
MCARI	$[((\text{RedEdge} - \text{RED}) - (0.2(\text{RedEdge} + \text{Green})](\frac{RedEdge}{RED})$	[7] (Daughtry, 2000)

2.3. Statistical Analysis

All statistical analyses were performed in the SPSS statistical software (IBM SPSS Statistics v27.0.1.0). Initially, descriptive statistics were calculated for each variable to summarize the data distribution across treatments. One-way analysis of variance (ANOVA) was conducted to assess the effect of treatments on the measured parameters. Turkey's HSD post hoc test was then used for pair-wise comparisons, where significant differences were detected ($p < 0.05$). The assumptions of normality and homogeneity were tested prior to conducting the analysis of variance (ANOVA).

3. Results

3.1. Soil Properties of the Studied Soil

The physicochemical characteristics of the soil are summarized in Table 2. Baseline values were established at the beginning of the experiment (November 2022) to provide a reference for evaluating treatment effects over time. The soil was initially classified as clay loam, with a satisfactory nutrient status indicative of prior adequate fertilization. At the starting time, the mean soil pH was recorded at 7.96. By the end of the experimental period (May 2025), a slight decline in pH values was observed across all treatments. The highest pH at the final stage was found in the control (C) at 7.82, while fertilized plots exhibited slightly lower values of 7.73, 7.78, and 7.76 for treatments U, U+UI, and U+NI, respectively. In contrast, EC demonstrated a clear increasing trend, among all the treatments, throughout the study. Initial EC values averaged 219 µS/cm, increasing by the end of the trial to 485 µS/cm (U), 522 µS/cm (U+UI), and 553 µS/cm (U+NI). For the remaining soil parameters, no statistically significant differences were detected between treatments. Most nutrients showed a natural declining trend over time, likely due to plant uptake and the absence of additional nutrient inputs during the experimental period.

Table 2. Soil Properties from the experimental field.

Soil Properties		pH	EC	SOM	N	P	K	Fe	Cu	Mn	Zn
Baseline		7.96	219	2.54	0.19	30.65	285.00	4.56	8.94	12.77	8.41
Season 2024–2025	**C**	7.82	474	2.50	0.17	27.20	207.80	4.12	8.45	11.56	8.45
	U	7.73	485	2.51	0.19	22.85	211.10	3.96	8.26	12.36	8.22
	U+NI	7.78	522	2.48	0.20	23.07	216.40	4.05	8.32	12.04	8.17
	U+UI	7.76	553	2.46	0.21	22.13	225.00	4.10	8.56	11.78	8.34

Table details: Soil pH measured in a 1:1 soil-water ratio; EC: (µS/cm); SOM: (%); Exchangeable K: (mg/kg); Total-N: (%); P: (mg/kg); Fe, Cu, Mn, Zn: (mg/kg).

3.2. Growing Degree Days (GDDs)

The accumulation of GDDs was monitored across all phenological stages of Tritordeum during three consecutive growing seasons [43]. GDD values were consistent throughout the years, indicating relatively stable thermal conditions throughout the experimental period (Table 3). During the emergence stage (BBCH 00–19), GDDs ranged from 127.60 to 130.45, while in the tillering stage (BBCH 20–29), values remained steady around 370 GDDs across all seasons. The stem elongation stage (BBCH 30–39) occurred at around 597.80–598.30 GDDs. Flowering (BBCH 60–69) was consistently observed from 807.20 to 810.50 GDDs, followed by Seed Filling (BBCH 70–79) around 1072.40–1078.05 GDDs. More variation was observed during the ripening stage (BBCH 80–89), where GDDs ranged from 1430.40 to 1479.05. The senescence stage (BBCH 90–99) recorded the highest cumulative GDDs, with values ranging from 1606.45 to 1795.35, indicating differences in the length of the final phenological phase across years. Overall, the observed stability in GDD accumulation up to flowering reflects consistent thermal conditions critical for early crop development, while slight differences in the ripening and senescence stages suggest potential variability in late-season temperature regimes.

Table 3. Growing degree days (GDDs) during the experimental period (2022–2025) [43].

Growing Season	2022–2023	2023–2024	2024–2025
Emergence [BBCH 00–19]	127.60	129.65	130.45
Tillering [BBCH 20–29]	373.15	369.45	370.80
Stem Elongation [BBCH 30–39]	597.80	597.00	598.30
Flowering [BBCH 60–69]	811.15	807.20	810.50
Seed Filling [BBCH 70–79]	1077.05	1072.40	1078.05
Ripening [BBCH 80–89]	1430.40	1479.05	1449.15
Senescence [BBCH 90–99]	1617.20	1795.35	1606.45

3.3. Effect of Different Types of N Fertilization on Agronomic Characteristics

Agronomic traits recorded during the tillering stage (BBCH 20–29) are presented in Table 4. Plant height exhibited statistically significant differences among treatments only in the 2024 season ($F = 6.973$, $p < 0.05$), where fertilization significantly influenced growth. Plants treated with a nitrification inhibitor (24.50 $\pm$ 0.85 cm), urease inhibitor (23.68 $\pm$ 1.10 cm), and urea (23.78 $\pm$ 1.22 cm) were significantly taller than those in the control treatment (21.02 $\pm$ 1.39 cm). In 2023 and 2025, differences in plant height among treatments were not statistically significant; however, higher mean values were consistently observed under the EEF treatments. Fresh weight showed no significant variation across treatments in any year; nevertheless, numerically higher values were recorded in the U+UI and U+NI plots in both 2024 (1.66 $\pm$ 0.46 g and 1.46 $\pm$ 0.22 g, respectively) and 2025 (0.665 $\pm$ 0.035 g and 0.665 $\pm$ 0.167 g, respectively).

In contrast, agronomic traits recorded at the stem elongation stage (BBCH 30–39) (Table 5) showed significant differences in plant height across all three growing seasons. EEFs consistently demonstrated superior performance in promoting plant height compared to both the urea and control treatments. In 2023, the highest height of plants was recorded under the nitrification inhibitor treatment (36.208 $\pm$ 1.213 cm), while in 2024, the tallest plants were observed in the urease inhibitor treatment (47.108 $\pm$ 1.014 cm). In 2025, U+NI again resulted in the greatest height (33.050 $\pm$ 1.801 cm). Fresh weight did not show significant variation among treatments in any year; however, numerically higher values were again observed in the fertilized treatments compared to the control.

Table 4. Agronomic characteristics on Tillering [BBCH 20–29].

Tillering [BBCH 20–29]					
	Treatment	**C**	**U**	**U+NI**	**U+UI**
Mean ± SD 2023	Height	23.433 ± 1.159	23.673 ± 1.780	25.268 ± 1.464	25.000 ± 1.284
	F	1.646 ns			
	Fresh Weight	1.192 ± 0.220	1.155 ± 0.132	1.367 ± 0.280	1.234 ± 0.082
	F	0.907 ns			
Mean ± SD 2024	Height	21.017 ± 1.394 a	23.775 ± 1.220 b	24.500 ± 0.850 b	23.683 ± 1.101 b
	F	6.973 *			
	Fresh Weight	1.390 ± 0.383	1.314 ± 0.394	1.457 ± 0.225	1.665 ± 0.458
	F	0.646 ns			
Mean ± SD 2025	Height	15.025 ± 0.791	16.050 ± 0.775	15.050 ± 0.795	15.150 ± 2.293
	F	0.541 ns			
	Fresh Weight	0.628 ± 0.061	0.656 ± 0.165	0.665 ± 0.167	0.665 ± 0.035
	F	0.079 ns			

Table details: height: (cm), fresh weight: (g), ns: not significant. Different letters (a, b) mark significant differences among treatments within a row at the 5% level; identical or shared letters indicate no difference. F—fertilisation shows the ANOVA F-statistics for fertilisation effects, with asterisks indicating significance (* $p < 0.01$).

Table 5. Agronomic characteristics on Stem Elongation [BBCH 30–39].

Stem Elongation [BBCH 30–39]					
	Treatment	**C**	**U**	**U+NI**	**U+UI**
Mean ± SD 2023	Height	28.158 ± 1.977 a	31.942 ± 1.947 b	32.692 ± 0.394 b	36.208 ± 1.213 c
	F	12.463 *			
	Fresh Weight	2.506 ± 0.197	2.550 ± 0.202	2.632 ± 0.000	2.526 ± 0.426
	F	0.102 ns			
Mean ± SD 2024	Height	33.475 ± 1.229 a	43.018 ± 1.068 b	47.108 ± 1.014 c	43.700 ± 1.909 b
	F	74.699 ***			
	Fresh Weight	4.874 ± 0.411	5.123 ± 1.067	5.130 ± 1.164	4.488 ± 0.501
	F	0.500 ns			
Mean ± SD 2025	Height	27.983 ± 1.601 a	32.742 ± 2.113 b	30.950 ± 0.923 ab	33.050 ± 1.801 b
	F	7.771 *			
	Fresh Weight	3.168 ± 0.135 a	3.500 ± 0.098 b	4.041 ± 0.174 c	3.782 ± 0.216 bc
	F	21.490 **			

Table details: height: (cm), fresh weight: (g), ns: not significant. Different letters (a, b, c, bc, ab) mark significant differences among treatments within a row at the 5% level; identical or shared letters indicate no difference. F—fertilisation shows the ANOVA F-statistics for fertilisation effects, with asterisks indicating significance (* $p < 0.01$, ** $p < 0.001$, *** $p < 0.0001$).

Agronomic characteristics recorded during the flowering stage (BBCH 60–69) are presented in Table 6, where significant differences in plant height were observed across all three growing seasons between the fertilized treatments and the control. EEFs generally produced taller plants than the urea treatment, although no statistically significant differences were found among the fertilized treatments themselves. In 2023, the tallest plants were recorded under the urease inhibitor treatment (62.883 ± 2.400 cm), while in 2024 and 2025, the nitrification inhibitor treatment resulted in the highest plant height values (78.151 ± 1.949 cm and 78.067 ± 1.156 cm, respectively). Fresh weight exhibited significant variation only in 2025, during which the inhibitor-based treatments outperformed the others (U+UI: 12.386 ± 1.252 g; U+NI: 11.217 ± 2.330 g).

Table 6. Agronomic characteristics on Flowering [BBCH 60–69].

Flowering [BBCH 60–69]					
	Treatment	**C**	**U**	**U+NI**	**U+UI**
Mean ± SD 2023	Height	55.208 ± 2.878 a	60.925 ± 1.820 b	60.574 ± 2.661 b	62.883 ± 2.400 b
	F	7.075 *			
	Fresh Weight	8.895 ± 0.762	9.904 ± 0.767	9.649 ± 0.723	9.510 ± 1.140
	F	0.983 ns			
Mean ± SD 2024	Height	65.205 ± 1.606 a	74.905 ± 1.701 b	78.151 ± 1.949 b	77.232 ± 1.516 b
	F	48.761 ***			
	Fresh Weight	11.721 ± 1.770	13.271 ± 1.222	12.599 ± 1.475	13.985 ± 0.956
	F	1.932 ns			
Mean ± SD 2025	Height	66.508 ± 1.425 a	73.125 ± 1.243 b	78.067 ± 1.156 c	73.658 ± 1.658 b
	F	47.456 ***			
	Fresh Weight	8.356 ± 1.899 a	10.263 ± 2.008 ab	11.217 ± 2.330 ab	12.386 ± 1.252 b
	F	3.175 *			

Table details: height: (cm), fresh weight: (g), ns: not significant. Different letters (a, b, ab, c) mark significant differences among treatments within a row at the 5% level; identical or shared letters indicate no difference. F—fertilisation shows the ANOVA F-statistics for fertilisation effects, with asterisks indicating significance (* $p < 0.01$, *** $p < 0.0001$).

Similarly, the agronomic traits at the seed filling stage (BBCH 70–79), presented in Table 7, revealed consistent and significant differences in both plant height and fresh weight across all three years. Plants in the control plots had significantly lower height compared to the fertilized treatments, with EEFs again promoting greater height than standard urea. Specifically, the urease inhibitor treatment produced the tallest plants in 2023 (84.292 ± 2.279 cm) and 2024 (92.833 ± 2.285 cm), while in 2025, the highest value was observed under the nitrification inhibitor treatment (85.117 ± 1.168 cm). Regarding fresh weight, significant differences were recorded in the first two seasons, with the urea (2023: 15.173 ± 2.227 g; 2024: 15.225 ± 0.497 g) and urease inhibitor treatments (2023: 14.456 ± 0.812 g; 2024: 15.493 ± 1.494 g) demonstrating more favorable performance.

Agronomic traits during the ripening (BBCH 80–89) and senescence (BBCH 90–99) stages, summarized in Table 8, showed significant differences among treatments throughout the three-year study. For the plant height, in 2023, the highest value was observed under the U+UI treatment (73.705 ± 1.770 cm), while in 2024 and 2025, the greatest heights were found in the U+NI treatment (82.000 ± 1.639 cm and 75.900 ± 2.156 cm, respectively). Fresh weight exhibited significant variation during the first two years, but not in the final season. In 2023, the highest fresh weight was recorded under the urea treatment (11.627 ± 0.884 g), whereas in 2024, the U+UI treatment yielded the maximum value (14.733 ± 1.390 g). Spike length showed significant differences only during the first growing season, with the best result observed in the U+NI treatment (8.858 ± 0.637 cm). Although no significant differences were found in 2024 and 2025, the numerically highest values were recorded under U+UI (9.250 ± 0.167 cm) and urea (8.917 ± 0.399 cm), respectively.

3.4. Effect of Different Types of N Fertilization on Multispectral Indices

VIs obtained from UAV imagery at the tillering (BBCH 20–29) stage are presented in Table 9. At tillering, significant treatment differences were observed in the 2023 season for GNDVI ($F = 4.268$, $p < 0.05$), NDRE ($F = 3.078$, $p < 0.05$), and NDVI ($F = 5.013$, $p < 0.01$). In this year, the highest GNDVI was recorded under the control (0.548), while the U+NI treatment showed the highest NDRE (0.181) and NDVI (0.665) values. During 2024, only NDRE displayed significant variation ($F = 3.137$, $p < 0.05$), with the urea treatment (U)

reaching the maximum value (0.231). No significant differences were detected among treatments in any index in 2025.

Table 7. Agronomic characteristics on Seed Filling [BBCH 70–79].

Seed Filling [BBCH 70–79]					
	Treatment	**C**	**U**	**U+NI**	**U+UI**
Mean ± SD 2023	Height	64.833 ± 2.704 a	74.317 ± 2.745 b	79.230 ± 1.725 c	84.292 ± 2.279 d
	F	47.808 **			
	Fresh Weight	9.118 ± 0.669 a	15.173 ± 2.227 c	12.633 ± 0.531 b	14.456 ± 0.812 bc
	F	18.450 **			
Mean ± SD 2024	Height	72.483 ± 1.569 a	83.418 ± 2.131 b	87.633 ± 1.666 c	92.833 ± 2.285 d
	F	79.701 ***			
	Fresh Weight	10.925 ± 1.103 a	15.225 ± 0.497 b	13.598 ± 1.729 b	15.493 ± 1.494 b
	F	10.531 *			
Mean ± SD 2025	Height	73.942 ± 3.163 a	79.815 ± 2.628 b	85.117 ± 1.168 c	82.542 ± 1.980 bc
	F	16.548 ***			
	Fresh Weight	10.498 ± 1.081	12.658 ± 1.375	13.963 ± 2.503	13.545 ± 1.271
	F	3.489 ns			

Table details: height: (cm), fresh weight: (g), ns: not significant. Different letters (a, b, c, d, bc) mark significant differences among treatments within a row at the 5% level; identical or shared letters indicate no difference. F—fertilisation shows the ANOVA F-statistics for fertilisation effects, with asterisks indicating significance (* $p < 0.01$, ** $p < 0.001$, *** $p < 0.0001$).

Table 8. Agronomic characteristics on Ripening [BBCH 80–89]—Senescence [BBCH 90–99].

Ripening [BBCH 80–89]—Senescence [BBCH 90–99]					
	Treatment	**C**	**U**	**U+NI**	**U+UI**
Mean ± SD 2023	Height	64.833 ± 2.704 a	71.534 ± 2.703 b	72.115 ± 1.799 b	73.705 ± 1.770 b
	F	27.728 **			
	Fresh Weight	9.118 ± 0.669 a	11.627 ± 0.884 b	10.174 ± 0.687 b	11.354 ± 1.076 b
	F	25.937 **			
	Spike Length	7.068 ± 0.302 a	8.500 ± 0.782 b	8.858 ± 0.637 b	8.792 ± 0.629 b
	F	7.490 *			
Mean ± SD 2024	Height	68.417 ± 2.217 a	77.875 ± 1.259 b	82.000 ± 1.639 c	81.658 ± 1.948 c
	F	49.383 **			
	Fresh Weight	8.298 ± 0.408 a	13.358 ± 1.519 bc	11.388 ± 1.182 b	14.733 ± 1.390 c
	F	21.489 **			
	Spike Length	8.333 ± 0.471	9.125 ± 0.599	9.167 ± 0.430	9.250 ± 0.167
	F	3.671 ns			
Mean ± SD 2025	Height	66.989 ± 1.932 a	73.067 ± 3.113 b	75.900 ± 2.156 b	73.525 ± 0.856 b
	F	12.262 *			
	Fresh Weight	9.555 ± 1.721	11.003 ± 2.374	12.185 ± 2.337	11.783 ± 3.076
	F	0.915 ns			
	Spike Length	8.875 ± 0.831	8.917 ± 0.399	8.232 ± 0.136	8.217 ± 0.382
	F	2.376 ns			

Table details: height: (cm), fresh weight: (g), ns: not significant. Different letters (a, b, c, bc) mark significant differences among treatments within a row at the 5% level; identical or shared letters indicate no difference. F—fertilisation shows the ANOVA F-statistics for fertilisation effects, with asterisks indicating significance (* $p < 0.01$, ** $p < 0.001$).

At stem elongation (BBCH 30–39) stage (Table 10), VIs exhibited limited response to fertilisation strategies. NDVI was the only index significantly affected, both in 2024 (F = 2.824,

$p < 0.05$) and in 2023 (F = 2.850, ns but close to significance). In 2024, NDVI peaked under the U treatment (0.903), while in 2025 the highest NDVI value was observed under U+NI (0.899). GNDVI, MCARI, and NDRE did not vary significantly across treatments in any of the three growing seasons.

VIs during the flowering stage (BBCH 60–69) are presented in Table 11. No significant differences were observed among treatments in 2023 for any VI. In contrast, during 2024, GNDVI (F = 16.077, $p < 0.001$), NDRE (F = 17.296, $p < 0.001$), and NDVI (F = 14.871, $p < 0.001$) showed statistically significant treatment effects. The highest GNDVI value was recorded under the U treatment (0.802), while the lowest was observed in U+NI (0.761). NDRE peaked in the U treatment (0.422), and NDVI ranged from 0.892 (U+NI) to 0.914 (U). In 2025, treatment effects remained significant for GNDVI (F = 3.109, $p < 0.05$) and NDVI (F = 4.267, $p < 0.01$), but not for MCARI or NDRE. U+NI resulted in the highest GNDVI (0.777) and NDVI (0.882), while U+UI had the lowest values for both indices.

At the seed filling stage (BBCH 70–79) (Table 12), all VIs were non-significant in 2023. In 2024, only MCARI (F = 5.189, $p < 0.01$) and NDVI (F = 4.735, $p < 0.01$) showed significant differences. The highest values for both indices were recorded in the U+NI treatment (NDVI: 0.620; MCARI: 0.475), while the lowest values were observed in U+UI (MCARI: 0.416; NDVI: 0.577) and U (MCARI: 0.415; NDVI: 0.578). In 2025, all four indices were significantly affected by fertilisation: GNDVI (F = 8.545, $p < 0.001$), MCARI (F = 6.698, $p < 0.001$), NDRE (F = 8.688, $p < 0.001$), and NDVI (F = 10.616, $p < 0.001$). For this final season, U+NI consistently produced the highest values across all indices (e.g., GNDVI: 0.637; NDVI: 0.696), while U+UI recorded the lowest values for most indices, particularly NDVI (0.593).

VIs during the ripening (BBCH 80–89) and senescence (BBCH 90–99) stages are presented in Table 13. In the 2023 season, no statistically significant differences were observed for any of the VIs across treatments. In the 2024 season, GNDVI (F = 3.932, $p < 0.01$) and NDVI (F = 17.072, $p < 0.01$) exhibited significant treatment effects. GNDVI values ranged from 0.359 in U+NI to 0.386 in U. NDVI peaked under control (0.249), whereas U recorded the lowest value (0.069). During the 2025 season, all indices were significantly affected by the fertilisation treatments. GNDVI (F = 6.126, $p < 0.001$) was highest under U+NI (0.358), while U+UI recorded the lowest value (0.315). MCARI (F = 7.240, $p < 0.001$) showed maximum values in U+NI (0.070) and minimum in U+UI (0.036). NDRE was also significantly influenced (F = 5.424, $p < 0.01$), with U+NI exhibiting the highest value (0.059) and U+UI the lowest (0.041). Finally, NDVI (F = 30.932, $p < 0.001$) demonstrated the most pronounced differences, peaking at 0.204 under U+NI and declining to 0.165 under U+UI.

3.5. Effect of Different Types of N Fertilization on Qualitative Characteristics

Grain yield is presented in Table 14. As expected, the lowest yield values were consistently recorded in the control treatment across all three years, reflecting the absence of fertilization. A declining trend in control plot yields was observed over time, with the highest value in 2023 (2031.963 ± 36.117 kg/ha) and the lowest in 2025 (1839.063 ± 35.950 kg/ha). Fertilization significantly affected grain yield in all years of the study. In 2023 and 2024, the highest yields were recorded under the urea treatment (2390.263 ± 42.828 kg/ha and 1366.000 ± 45.598 kg/ha, respectively). The urea + nitrification inhibitor (U+NI) treatment also performed well, showing the second-highest yield values in those years (2180.450 ± 41.850 kg/ha in 2023 and 1208.998 ± 43.414 kg/ha in 2024). In contrast, during the 2025 season, the highest yield was recorded under the U+NI treatment (2319.050 ± 41.652 kg/ha), surpassing all other treatments.

Table 9. Multispectral vegetation indices on Tillering [BBCH 20–29].

Tillering [BBCH 20–29]																
Index	**GNDVI**				**MCARI**				**NDRE**				**NDVI**			
Treatment	**C**	**U**	**U+NI**	**U+UI**	**C**	**U**	**U+NI**	**U+UI**	**C**	**U**	**U+NI**	**U+UI**	**C**	**U**	**U+NI**	**U+UI**
Mean ± SD 2023	0.548 ± 0.011 b	0.502 ± 0.010 a	0.543 ± 0.012 ab	0.505 ± 0.013 a	0.540 ± 0.016	0.479 ± 0.016	0.531 ± 0.018	0.491 ± 0.020	0.178 ± 0.006 ab	0.157 ± 0.006 a	0.181 ± 0.007 b	0.165 ± 0.007 ab	0.683 ± 0.015 b	0.617 ± 0.013 a	0.665 ± 0.016 ab	0.613 ± 0.018 a
F	4.268 *				2.859 ns				3.078 *				5.013 **			
Mean ± SD 2024	0.626 ± 0.006	0.635 ± 0.007	0.627 ± 0.007	0.617 ± 0.008	0.526 ± 0.012	0.479 ± 0.013	0.489 ± 0.014	0.485 ± 0.013	0.217 ± 0.004 ab	0.231 ± 0.005 c	0.224 ± 0.005 ab	0.214 ± 0.005 a	0.809 ± 0.006	0.815 ± 0.008	0.814 ± 0.008	0.798 ± 0.009
F	1.116 ns				2.657 ns				3.137 *				0.965 ns			
Mean ± SD 2025	0.367 ± 0.009	0.367 ± 0.009	0.367 ± 0.011	0.383 ± 0.010	0.340 ± 0.014	0.357 ± 0.013	0.329 ± 0.015	0.351 ± 0.014	0.078 ± 0.004	0.076 ± 0.004	0.078 ± 0.005	0.086 ± 0.005	0.451 ± 0.015	0.469 ± 0.014	0.466 ± 0.016	0.489 ± 0.015
F	0.593 ns				0.783 ns				0.960 ns				1.061 ns			

Table details: ns: not significant, Different letters (a, b, c, ab) mark significant differences among treatments within a row at the 5% level; identical or shared letters indicate no difference. F—fertilisation shows the ANOVA F-statistics for fertilisation effects, with asterisks indicating significance (* $p < 0.01$, ** $p < 0.001$).

Table 10. Multispectral vegetation indices on Stem Elongation [BBCH 30–39].

Stem Elongation [BBCH 30–39]																
Index	**GNDVI**				**MCARI**				**NDRE**				**NDVI**			
Treatment	**C**	**U**	**U+NI**	**U+UI**	**C**	**U**	**U+NI**	**U+UI**	**C**	**U**	**U+NI**	**U+UI**	**C**	**U**	**U+NI**	**U+UI**
Mean ± SD 2023	0.733 ± 0.004	0.738 ± 0.005	0.723 ± 0.005	0.722 ± 0.006	0.613 ± 0.014	0.651 ± 0.014	0.611 ± 0.013	0.614 ± 0.013	0.288 ± 0.004	0.294 ± 0.005	0.291 ± 0.004	0.285 ± 0.005	0.879 ± 0.003	0.887 ± 0.003	0.874 ± 0.003	0.874 ± 0.005
F	2.517 ns				1.993 ns				0.780 ns				2.850 ns			
Mean ± SD 2024	0.764 ± 0.003	0.768 ± 0.003	0.763 ± 0.003	0.759 ± 0.004	0.980 ± 0.010	0.986 ± 0.011	1.005 ± 0.013	0.989 ± 0.013	0.367 ± 0.003	0.374 ± 0.004	0.365 ± 0.004	0.361 ± 0.004	0.900 ± 0.002 ab	0.903 ± 0.002 b	0.902 ± 0.002 ab	0.895 ± 0.003 a
F	1.176 ns				0.997 ns				2.234 ns				2.824 *			
Mean ± SD 2025	0.746 ± 0.007	0.751 ± 0.005	0.758 ± 0.006	0.746 ± 0.005	0.878 ± 0.000	0.877 ± 0.012	0.875 ± 0.013	0.862 ± 0.011	0.339 ± 0.007	0.348 ± 0.005	0.353 ± 0.005	0.346 ± 0.005	0.891 ± 0.015	0.893 ± 0.005	0.899 ± 0.005	0.890 ± 0.004
F	0.999 ns				0.401 ns				1.321 ns				0.802 ns			

Table details: ns: not significant, Different letters (a, b, ab) mark significant differences among treatments within a row at the 5% level; identical or shared letters indicate no difference. F—fertilisation shows the ANOVA F-statistics for fertilisation effects, with asterisks indicating significance (* $p < 0.01$).

Table 11. Multispectral vegetation indices on Flowering [BBCH 60–69].

Flowering [BBCH 60–69]																
Index	**GNDVI**				**MCARI**				**NDRE**				**NDVI**			
Treatment	**C**	**U**	**U+NI**	**U+UI**	**C**	**U**	**U+NI**	**U+UI**	**C**	**U**	**U+NI**	**U+UI**	**C**	**U**	**U+NI**	**U+UI**
Mean ± SD 2023	0.744 ± 0.005	0.751 ± 0.005	0.741 ± 0.005	0.745 ± 0.006	0.841 ± 0.014	0.871 ± 0.015	0.828 ± 0.014	0.841 ± 0.014	0.355 ± 0.005	0.356 ± 0.005	0.355 ± 0.005	0.349 ± 0.008	0.875 ± 0.003	0.875 ± 0.003	0.873 ± 0.003	0.869 ± 0.004
F	0.596 ns				1.635 ns				0.248 ns				0.805 ns			
Mean ± SD 2024	0.799 ± 0.004 bc	0.802 ± 0.004 c	0.761 ± 0.006 a	0.785 ± 0.005 b	0.923 ± 0.012	0.936 ± 0.011	0.947 ± 0.015	0.924 ± 0.012	0.417 ± 0.005 bc	0.422 ± 0.005 c	0.370 ± 0.007 a	0.400 ± 0.006 b	0.912 ± 0.002 b	0.914 ± 0.002 b	0.892 ± 0.003 a	0.906 ± 0.002 b
F	16.077 ***				0.777 ns				17.296 ***				14.871 ***			
Mean ± SD 2025	0.766 ± 0.006 ab	0.767 ± 0.007 ab	0.777 ± 0.007 b	0.749 ± 0.007 a	0.786 ± 0.014	0.778 ± 0.015	0.799 ± 0.016	0.770 ± 0.017	0.399 ± 0.006	0.403 ± 0.006	0.411 ± 0.006	0.388 ± 0.006	0.871 ± 0.005 ab	0.868 ± 0.006 ab	0.882 ± 0.006 b	0.852 ± 0.007 a
F	3.109 *				0.613 ns				2.529 ns				4.267 **			

Table details: ns: not significant, Different letters (a, b, c, bc, ab) mark significant differences among treatments within a row at the 5% level; identical or shared letters indicate no difference. F—fertilisation shows the ANOVA F-statistics for fertilisation effects, with asterisks indicating significance (* $p < 0.01$, ** $p < 0.001$, *** $p < 0.0001$).

Table 12. Multispectral vegetation indices on Seed Filling [BBCH 70–79].

Seed Filling [BBCH 70–79]																
Index	**GNDVI**				**MCARI**				**NDRE**				**NDVI**			
Treatment	**C**	**U**	**U+NI**	**U+UI**	**C**	**U**	**U+NI**	**U+UI**	**C**	**U**	**U+NI**	**U+UI**	**C**	**U**	**U+NI**	**U+UI**
Mean ± SD 2023	0.554 ± 0.008	0.560 ± 0.007	0.563 ± 0.007	0.546 ± 0.008	0.444 ± 0.016	0.406 ± 0.015	0.441 ± 0.015	0.435 ± 0.016	0.197 ± 0.005	0.201 ± 0.005	0.212 ± 0.004	0.196 ± 0.005	0.559 ± 0.010	0.548 ± 0.010	0.579 ± 0.009	0.551 ± 0.011
F	1.013 ns				1.285 ns				2.088 ns				2.108 ns			
Mean ± SD 2024	0.577 ± 0.007	0.579 ± 0.006	0.590 ± 0.007	0.569 ± 0.007	0.454 ± 0.013 ab	0.415 ± 0.013 a	0.475 ± 0.014 b	0.416 ± 0.012 a	0.226 ± 0.005	0.219 ± 0.004	0.226 ± 0.005	0.214 ± 0.005	0.600 ± 0.009 ab	0.578 ± 0.009 a	0.620 ± 0.010 b	0.577 ± 0.010 a
F	1.747 ns				5.189 **				5.889 ns				4.735 **			
Mean ± SD 2025	0.605 ± 0.009 b	0.606 ± 0.009 b	0.637 ± 0.008 c	0.575 ± 0.009 a	0.663 ± 0.017 b	0.658 ± 0.019 b	0.706 ± 0.019 b	0.591 ± 0.019 a	0.257 ± 0.007 b	0.259 ± 0.007 b	0.280 ± 0.007 b	0.229 ± 0.007 a	0.641 ± 0.012 b	0.633 ± 0.013 ab	0.696 ± 0.013 c	0.593 ± 0.014 a
F	8.545 ***				6.698 ***				8.688 ***				10.616 ***			

Table details: ns: not significant, Different letters (a, b, c, ab) mark significant differences among treatments within a row at the 5% level; identical or shared letters indicate no difference. F—fertilisation shows the ANOVA F-statistics for fertilisation effects, with asterisks indicating significance (** $p < 0.001$, *** $p < 0.0001$).

Table 13. Multispectral vegetation indices on Ripening [BBCH 80–89]—Senescence [BBCH 90–99].

Ripening [BBCH 80–89]—Senescence [BBCH 90–99]																
Index	**GNDVI**				**MCARI**				**NDRE**				**NDVI**			
Treatment	**C**	**U**	**U+NI**	**U+UI**	**C**	**U**	**U+NI**	**U+UI**	**C**	**U**	**U+NI**	**U+UI**	**C**	**U**	**U+NI**	**U+UI**
Mean ± SD 2023	0.321 ± 0.006	0.318 ± 0.006	0.325 ± 0.006	0.317 ± 0.006	0.054 ± 0.004	0.052 ± 0.004	0.058 ± 0.003	0.051 ± 0.004	0.060 ± 0.003	0.058 ± 0.003	0.061 ± 0.003	0.054 ± 0.003	0.190 ± 0.005	0.186 ± 0.005	0.194 ± 0.004	0.183 ± 0.005
F	0.453 ns				0.739 ns				1.076 ns				1.125 ns			
Mean ± SD 2024	0.384 ± 0.066 b	0.386 ± 0.006 b	0.359 ± 0.008 a	0.381 ± 0.005 b	0.059 ± 0.038	0.059 ± 0.006	0.059 ± 0.005	0.054 ± 0.003	0.071 ± 0.029	0.069 ± 0.003	0.069 ± 0.003	0.067 ± 0.002	0.249 ± 0.082 b	0.207 ± 0.005 a	0.199 ± 0.006 a	0.204 ± 0.004 a
F	3.932 **				2.234 ns				0.307 ns				17.072 **			
Mean ± SD 2025	0.342 ± 0.008 b	0.343 ± 0.007 b	0.358 ± 0.007 b	0.315 ± 0.007 a	0.049 ± 0.005 ab	0.056 ± 0.006 bc	0.070 ± 0.006 c	0.036 ± 0.004 a	0.047 ± 0.003 a	0.052 ± 0.003 ab	0.059 ± 0.003 b	0.041 ± 0.003 a	0.184 ± 0.006 bc	0.088 ± 0.016 a	0.204 ± 0.006 c	0.165 ± 0.005 b
F	6.126 ***				7.240 ***				5.424 **				30.932 ***			

Table details: ns: not significant Different letters (a, b, c, bc, ab) mark significant differences among treatments within a row at the 5% level; identical or shared letters indicate no difference. F—fertilisation shows the ANOVA F-statistics for fertilisation effects, with asterisks indicating significance (** $p < 0.001$, *** $p < 0.0001$).

Table 14. Qualitative Characteristics during the experimental period.

Treat.	**Yield (kg/ha)**				**Thousands Grain Weight (gr)**				**Protein Content (%)**			
	C	**U**	**U+NI**	**U+UI**	**C**	**U**	**U+NI**	**U+UI**	**C**	**U**	**U+NI**	**U+UI**
Mean ± SD 2023	2031.963 ± 36.117 a	2390.263 ± 42.828 c	2180.450 ± 41.857 b	2127.653 ± 41.022 b	30.400± 0.807 a	33.350 ± 0.854 b	33.700 ± 1.232 b	35.700 ± 0.830 c	12.409± 0.190 a	15.282 ± 0.531 b	14.943 ± 0.322 b	14.603 ± 0.751 b
F	55.852 ***				21.328 **				27.272 ***			
Mean ± SD 2024	1006.000 ± 29.998 ab	1366.000 ± 45.598 b	1208.998 ± 43.414 a	1079.000 ± 26.330 ab	33.667± 1.422	35.733± 1.364	35.867± 1.061	36.133± 1.422	12.797± 1.651 a	16.040± 0.591 b	15.178± 0.899 b	15.433± 0.257 b
F	71.993 ***				3.013 ns				8.211 **			
Mean ± SD 2025	1839.063 ± 35.950 a	2237.500 ± 39.114 b	2319.050 ± 41.652 c	2187.750 ± 40.267 b	30.923± 1.279	32.880± 1.775	33.358± 1.877	33.245± 0.758	12.668± 0.247 a	15.960± 0.533 b	15.521± 0.273 b	15.401± 0.113 b
F	115.903 ***				2.331 ns				83.125 ***			

Table details: Yield (kg/ha), thousand grain weight (g), and protein content (%). ns: not significant Different letters (a, b, c, ab) mark significant differences among treatments within a row at the 5% level; identical or shared letters indicate no difference. F—fertilisation shows the ANOVA F-statistics for fertilisation effects, with asterisks indicating significance (** $p < 0.001$, *** $p < 0.0001$).

TGW responded positively to fertilization, with both inhibitor treatments maintaining relatively stable and elevated values across all three years compared to the control. In 2023, the highest TGW was observed under the urease inhibitor treatment (U+UI: 35.700 ± 0.830 g), although no statistically significant differences were found among treatments in 2024 and 2025 (Table 14).

Protein content results are presented in Table 14. Protein content was significantly influenced by fertilization, with the control treatment consistently showing the lowest values across all three seasons. Urea-treated plots maintained higher protein percentages compared to treatments with inhibitors. Notably, the highest values were recorded under urea treatment in all years: 15.282 ± 0.531 in 2023, 16.040 ± 0.591 in 2024, and 15.960 ± 0.533 in 2025.

4. Discussion

4.1. Nitrogen Strategy Performance

Across all three growing seasons, N fertilisation had a pronounced effect on grain yield and protein content in Tritordeum, whereas TGW showed a more variable response. Compared to the control, all fertilised treatments (U, U+NI, and U+UI) significantly increased protein content each year. Despite some year-to-year variation, the control consistently exhibited the lowest protein levels, ranging from 12.41% to 12.80%, while fertilised treatments ranged from approximately 14.60% to 16.04% (Table 14), with no significant differences among the three N strategies. This outcome aligns with previous studies in wheat and barley [23,27,44].

Grain yield followed a similar pattern with all N treatments outperforming the control. The highest yields recorded under U and U+NI. Notably, U+NI surpassed both U and U+UI in 2025 (2319.05 kg/ha vs. 2237.50 and 2187.75 kg/ha, respectively), suggesting a potential cumulative benefit of nitrification inhibition over time. In contrast, yields in 2024 were markedly lower across all treatments (C: 1006.00 ± 29.998; U: 1366.00 ± 45.598; U+NI: 1208.99 ± 43.414; U+UI: 1079.00 ± 26.330), likely due to less favorable climatic conditions. Specifically, higher-than-optimal temperatures during critical growth stages in February and April, coupled with above-average precipitation in March, may have disrupted Tritordeum development by accelerating phenology, shortening grain filling, and increasing N losses, thereby reducing yield potential.

EEFs such as nitrification and urease inhibitors are designed to reduce N losses via volatilisation and leaching, potentially enhancing N availability during key growth phases. This mechanism may explain the improved yield performance of U+NI in the final year. However, no N-enhanced strategy (U+NI or U+UI) consistently and significantly outperformed conventional urea (U) across all years. These results partially reflect similar findings with other studies on maize and wheat, where EEFs have improved NUE and yield under specific conditions but not uniformly across environments or seasons [25,26]. In the context of Tritordeum, this outcome highlights the importance of environmental and temporal variability in EEF performance.

TGW exhibited limited variation among treatments and was not significantly affected by N strategy in 2024 or 2025. Although a slight numerical increase was observed under EEFs, these differences were inconsistent and not always statistically significant. This finding is consistent with research in durum wheat and other cereals, where TGW has been shown to be less responsive to N inputs than total yield or protein concentration [45,46]. TGW is often more strongly influenced by genotype and environmental stress during grain filling than by nutrient availability.

Overall, while all N applications improved yield and protein content relative to the control, EEF did not consistently outperform conventional urea. Nevertheless, the superior

yield performance of U+NI in 2025 suggests this strategy may offer agronomic advantages under Mediterranean conditions, particularly where N losses are elevated. Previous studies have shown that urease and nitrification inhibitors can enhance N uptake and reduce environmental losses when volatilisation and leaching risks are high [47,48], supporting these findings.

4.2. Temporal Response to EEFs

The responsiveness of Tritordeum to N treatments varied significantly across growth stages, with clearer agronomic and spectral differentiation observed from flowering onward. In early stages such as tillering and stem elongation, treatment effects were inconsistent. Plant height differences at tillering were only statistically significant in 2024 (Table 4), and fresh weight remained unaffected across all three years. Among VIs, NDVI, NDRE, and GNDVI showed significant differences during tillering in 2023, but this pattern was not sustained in subsequent seasons, suggesting limited diagnostic value of early-stage traits for N strategy discrimination. In contrast, the flowering and seed filling stages consistently revealed strong and significant treatment effects across both agronomic traits and VIs. In all three years, U+NI and U+UI treatments led to significantly taller plants than both the control and conventional urea, with U+NI consistently outperforming U+UI in height during flowering and seed filling. These stages coincide with peak N demand and vegetative expansion, amplifying treatment differentiation.

At seed filling, agronomic traits and UAV-derived indices showed treatment differentiation with varying significance across years. In 2023 and 2024, U+UI reached the highest plant height (84.3 cm and 92.8 cm, respectively), while fresh weight also peaked under U+UI in 2024 (15.49 g) (Table 7). In 2025, height differences remained significant, with U+NI reaching 85.1 cm, while fresh weight differences were not statistically significant. Among the VIs, NDVI and MCARI showed strong treatment differentiation in 2024 and 2025, with U+NI recording the highest NDVI (0.696) and MCARI (0.706) in 2025. These patterns suggest that U+NI effectively maintained canopy greenness and pigment content during peak N demand, while U+UI contributed more to height and biomass in earlier seasons, possibly due to rapid N availability following urease inhibition.

During ripening and senescence, treatment effects were more subdued, but meaningful differences emerged in both spectral and agronomic traits by the final season. In 2025, U+NI recorded the highest plant height (75.9 cm), fresh weight (12.2 g), NDVI (0.204), and MCARI (0.070), suggesting a more prolonged canopy function and better pigment retention (Tables 8 and 13). GNDVI and NDRE also supported this trend, with U+NI showing superior values. In contrast, 2023 and 2024 showed fewer significant differences, particularly for fresh weight and spike length, with most VIs showing either weak or non-significant separation. The emergence of clearer differences only in 2025 may reflect cumulative soil improvements or a more synchronized crop response under favorable weather, enabling the EEFs, especially the nitrification inhibitor, to better express their delayed N release potential during the final grain-filling period.

Collectively, these findings demonstrate that the response of Tritordeum to N strategies is highly stage-dependent, with the clearest treatment differentiation emerging from flowering onwards. U+NI consistently outperformed other treatments in sustaining canopy vigour and enhancing biomass accumulation, particularly during seed filling and late-season stages, likely due to the delayed nitrate availability conferred by nitrification inhibition. This aligns with studies in wheat and barley, where inhibitors have been shown to improve N synchrony with crop demand, reduce leaching, and support prolonged vegetative activity [49,50]. In contrast, U+UI showed stronger effects earlier in the cycle, especially in promoting height and fresh weight during the first two growing seasons,

consistent with its mode of action, which limits ammonia volatilisation and enhances early N uptake [51]. These temporal distinctions suggest that integrating both types of EEFs into a staged or combined strategy may optimise N availability across the growth cycle. Moreover, the robust agreement between UAV-derived indices (particularly NDVI, GNDVI, and MCARI) and ground-based traits reinforces their utility in detecting stage-specific N dynamics and guiding adaptive fertilisation management.

4.3. Remote Sensing Insight

The utilization of UAV-based spectral indices provided critical insight into the physiological responses of Tritordeum to N fertilisation strategies, thereby validating and complementing ground-based agronomic measurements. Despite the observed variability across years and stages, several VIs, particularly NDVI, GNDVI, and NDRE, demonstrated the ability to capture treatment-induced differences, especially under EEFs.

NDVI was the most consistent index across growth stages, with significant differences at multiple phenological stages, particularly at seed filling in 2025, when U+NI recorded the highest values, corresponding with greater plant height and fresh weight. Similar patterns during flowering and ripening in 2024 and 2025 further confirm NDVI's reliability as a proxy for canopy vigor and N status [52].

GNDVI, more sensitive to chlorophyll concentration, was especially effective at flowering and seed filling. In 2025, GNDVI differences were statistically significant, with the highest values under U+NI, mirroring patterns observed in NDVI and ground-based growth traits. Its responsiveness to N treatments at these stages highlights its potential for detecting subtle physiological changes in chlorophyll content before visible biomass differences emerge, as supported by previous work in cereal crops [53]. NDRE showed less consistent responses overall but was particularly effective in later stages (seed filling and ripening in 2025), thereby underscoring its efficacy in monitoring the late-season effects of N and the process of senescence within the canopy [42].

MCARI was less informative during early phenological stages (tillering, stem elongation). However, its sensitivity increased from the seed filling stage onward, particularly in 2024 and 2025, suggesting a delayed spectral response. This aligns with its sensitivity to pigment- and structure-related canopy changes later in the cycle [54]. MCARI was less stable across seasons, suggesting it is better suited as a supplementary rather than a primary indicator [55].

The observed correspondence between VIs dynamics and ground-based agronomic measurements supports the integration of UAV-based remote sensing into high-throughput phenotyping. Although absolute index sensitivity varied with year and phenological stage, likely due to environmental variability and crop development, the relative consistency in treatment ranking affirms their robustness. A multi-index approach is therefore recommended: NDVI for overall vigor, GNDVI for chlorophyll status, and NDRE for late-season physiological changes, with MCARI providing supplementary detail. Collectively, these indices quantified the impact of N fertilisation in Tritordeum and highlighted UAV sensing as a scalable tool for nutrient management in Mediterranean cropping systems.

4.4. Sustainability Implications

In this study, the three-year soil monitoring data provides valuable insights into the long-term sustainability of EEFs fertilisation strategies. By the end of the experiment (May 2025), a slight decline in soil pH was observed across all treatments. This acidification trend was more evident in fertilised plots, likely reflecting the cumulative effects of N transformations, particularly nitrification [56]. Nonetheless, all final pH values remained within agronomically acceptable ranges for Tritordeum cultivation. In contrast, EC increased

notably over time, especially in fertilised treatments. While the control plot recorded an endline EC of 374 µS/cm, values under urea, U+NI, and U+UI rose to 485, 522, and 553 µS/cm, respectively. These increases suggest a gradual accumulation of residual salts or fertilizer-derived ions in the root zone, particularly under EEF application. However, all EC values remained well below the salinity thresholds considered critical for cereal crops, indicating no immediate risk of salinization.

Total soil N remained stable or showed slight increases in fertilised plots. In contrast, the control exhibited a decline from 0.19% to 0.17% over the study period. This reduction, combined with a consistent downward trend in yield under the control, may point to a gradual depletion of soil fertility in the absence of N inputs. Conversely, minor increases in total N under U+NI and U+UI (to 0.20% and 0.21%, respectively) suggest improved N retention, potentially due to reduced losses via volatilisation or leaching, findings consistent with prior research on EEF performance [47]. Other macro- and micronutrients, including phosphorus (P), potassium (K), and micronutrients such as Fe, Cu, Mn, and Zn, generally declined across all treatments. These reductions are likely attributable to plant uptake over successive growing seasons, as no supplemental fertilisation of these elements was provided.

Overall, the use of EEFs did not negatively affect soil fertility and, in the case of total N, may have supported improved nutrient retention. While EC increased, it remained within acceptable limits. These findings underscore the potential of EEFs as a sustainable fertilisation strategy for the long term, contributing to both N efficiency and soil quality preservation.

4.5. Limitations and Future Research

Despite its multi-seasonal design and integration of agronomic and remote sensing data, this study presents some limitations. First, environmental conditions (e.g., rainfall, temperature) were not explicitly analyzed in relation to treatment performance, although they may have influenced N dynamics and crop development. Second, N loss pathways such as volatilisation, leaching, or gaseous emissions were not directly measured, limiting inferences on the environmental performance of EEFs. Third, the experiment was conducted on a single Tritordeum genotype and soil type, which may restrict the generalizability of findings to other varieties or agroecological zones.

Future research should incorporate N fate assessments, such as ammonia and N_2O emission measurements and nitrate leaching monitoring, to evaluate the full environmental impact of EEFs. Studies involving multiple Tritordeum genotypes and soil types, as well as rotational systems, would help confirm the robustness of the observed trends. Furthermore, integration of UAV-based sensing into real-time fertilisation models could enhance the applicability of these technologies in precision N management. Long-term trials should also explore how EEF strategies interact with climate variability and soil carbon dynamics to ensure both productivity and sustainability.

5. Conclusions

This three-year field study offers the first integrated assessment of Tritordeum's agronomic and physiological responses to N Fertilisation under Mediterranean conditions, using GDD-aligned phenological monitoring, UAV-derived multispectral indices, and soil fertility analysis. All N treatments significantly improved grain yield and protein content relative to the unfertilized control, confirming the crop's strong responsiveness to N inputs. By combining remote sensing and standard agronomic measurements across multiple seasons, this study provides a robust framework for evaluating N dynamics in

Tritordeum and contributes to the design of more sustainable fertilisation strategies in emerging Mediterranean cereals.

Although EEFs did not consistently outperform conventional urea across all years, U+NI demonstrated a cumulative agronomic advantage in the final season, likely due to sustained N availability and improved synchronization with crop demand. This delayed benefit may also reflect cumulative soil improvements and more favorable weather conditions in 2025, which enhanced the expression of the slow-release fertilizer effects. Temporal analysis revealed that treatment differentiation was most pronounced from flowering onwards, with U+NI consistently enhancing canopy greenness, biomass, and pigment content during seed filling and ripening. In contrast, U+UI showed stronger effects earlier in the cycle, particularly in promoting height and fresh weight, consistent with its role in enhancing early N uptake.

Multispectral indices showed strong alignment with ground-based traits and effectively captured treatment effects at stage-specific windows, confirming their utility in guiding adaptive fertilisation strategies. From a sustainability perspective, the EEFs supported N retention in soil without adversely affecting pH or salinity levels, and the minor increases in total soil N under U+NI and U+UI suggested reduced N losses.

Taken together, these findings highlight the stage-dependent efficacy of EEFs and support a dynamic fertilisation strategy tailored to phenological stages. Specifically, the use of urea combined with a nitrification inhibitor (U+NI) early in the season proved most effective in sustaining canopy vigor and improving yield and protein content, particularly from flowering through ripening. In contrast, urease inhibition (U+UI) showed greater influence on early biomass and height development. These results suggest that a split or combined application of both inhibitors, deploying U+NI at early stages and U+UI closer to peak vegetative growth, could optimize N synchrony, minimize losses, and enhance NUE under Mediterranean conditions. UAV-based remote sensing, when integrated with phenologically timed measurements, offers a scalable, non-invasive approach to implement and monitor N strategies. This framework supports more sustainable N management in Tritordeum and potentially other Mediterranean cereals.

Author Contributions: G.P.: Conceptualization, Methodology, Investigation, Data curation, Project administration, Writing—original draft, Writing—review & editing, Supervision; I.Z.: Investigation, Methodology, Resources, Formal analysis, Validation, Writing—original draft; E.G.: Methodology, Investigation, Data curation, Formal analysis, Visualization, Writing—original draft, Writing—review & editing; A.O.: Methodology, Investigation, Data curation, Formal analysis, Visualization, Writing—original draft, Writing—review & editing.; A.M.: Investigation, Formal analysis, Validation, Writing—review & editing; P.S.: Investigation, Data curation, Formal analysis, Validation, Writing—review & editing; I.K.: Conceptualization, Methodology, Validation, Writing—review & editing; S.F.: Conceptualization, Methodology, Resources, Supervision, Validation, Writing—review & editing; D.B.: Conceptualization, Methodology, Resources, Supervision, Validation, Writing—review & editing. All authors have read and agreed to the published version of the manuscript.

Funding: This research received no external funding.

Data Availability Statement: The data will be made available upon request.

Acknowledgments: During the preparation of this work, the authors used ChatGPT 4.0, an AI language model by OpenAI, to improve the language of the manuscript. After using this tool/service, the authors reviewed and edited the content as needed and take full responsibility for the content of the publication.

Conflicts of Interest: The authors declare that they have no known competing financial interests or personal relationships that could have appeared to influence the work reported in this paper.

Abbreviations

N	Nitrogen
NUE	Nitrogen Use Efficiency
EC	Electrical Conductivity
NBPT	N-(n-butyl) thiophosphoric triamide
EEFs	Enhanced-Efficiency Fertilisers
DCD	Dicyandiamide
NIs	Nitrification Inhibitors
SOM	Soil Organic Matter
DTPA	Diethylenetriaminepentaacetic Acid
VIs	Vegetation Indices
UAV	Unmanned Aerial Vehicles
GDS	Ground Sampling Distance

References

1. Ali, A.; Martelli, R.; Lupia, F.; Barbanti, L. Assessing Multiple Years' Spatial Variability of Crop Yields Using Satellite Vegetation Indices. *Remote Sens.* **2019**, *11*, 2384. [CrossRef]
2. Miller, J.O.; Shober, A.L.; Taraila, J. Assessing Relationships of Cover Crop Biomass and Nitrogen Content to Multispectral Imagery. *Agron. J.* **2024**, *116*, 1417–1427. [CrossRef]
3. Tilly, N.; Aasen, H.; Bareth, G. Fusion of Plant Height and Vegetation Indices for the Estimation of Barley Biomass. *Remote Sens.* **2015**, *7*, 11449–11480. [CrossRef]
4. Vidican, R.; Mălinaș, A.; Ranta, O.; Moldovan, C.; Marian, O.; Ghețe, A.; Ghișe, C.R.; Popovici, F.; Cătunescu, G.M. Using Remote Sensing Vegetation Indices for the Discrimination and Monitoring of Agricultural Crops: A Critical Review. *Agronomy* **2023**, *13*, 3040. [CrossRef]
5. Walsh, O.S.; Shafian, S.; Marshall, J.M.; Jackson, C.; McClintick-Chess, J.R.; Blanscet, S.M.; Swoboda, K.; Thompson, C.; Belmont, K.M.; Walsh, W.L. Assessment of UAV Based Vegetation Indices for Nitrogen Concentration Estimation in Spring Wheat. *Adv. Remote Sens.* **2018**, *07*, 71–90. [CrossRef]
6. Barnes, M.C.; Addai-Mensah, J.; Gerson, A.R. A Methodology for Quantifying Sodalite and Cancrinite Phase Mixtures and the Kinetics of the Sodalite to Cancrinite Phase Transformation. *Microporous Mesoporous Mater.* **1999**, *31*, 303–319. [CrossRef]
7. Daughtry, C. Estimating Corn Leaf Chlorophyll Concentration from Leaf and Canopy Reflectance. *Remote Sens. Environ.* **2000**, *74*, 229–239. [CrossRef]
8. Gitelson, A.A.; Kaufman, Y.J.; Merzlyak, M.N. Use of a Green Channel in Remote Sensing of Global Vegetation from EOS-MODIS. *Remote Sens. Environ.* **1996**, *58*, 289–298. [CrossRef]
9. Samborski, S.M.; Tremblay, N.; Fallon, E. Strategies to Make Use of Plant Sensors-Based Diagnostic Information for Nitrogen Recommendations. *Agron. J.* **2009**, *101*, 800–816. [CrossRef]
10. Lawlor, D.W.; Lemaire, G.; Gastal, F. Nitrogen, Plant Growth and Crop Yield. In *Plant Nitrogen*; Lea, P.J., Morot-Gaudry, J.-F., Eds.; Springer: Berlin/Heidelberg, Germany, 2001; pp. 343–367. ISBN 978-3-642-08731-8.
11. Rehman, H.U.; Alharby, H.F.; Al-Zahrani, H.S.; Bamagoos, A.A.; Alsulami, N.B.; Alabdallah, N.M.; Iqbal, T.; Wakeel, A. Enriching Urea with Nitrogen Inhibitors Improves Growth, N Uptake and Seed Yield in Quinoa (Chenopodium Quinoa Willd) Affecting Photochemical Efficiency and Nitrate Reductase Activity. *Plants* **2022**, *11*, 371. [CrossRef]
12. Bagheri, N. Development of a High-Resolution Aerial Remote-Sensing System for Precision Agriculture. *Int. J. Remote Sens.* **2017**, *38*, 2053–2065. [CrossRef]
13. Lu, N.; Wang, W.; Zhang, Q.; Li, D.; Yao, X.; Tian, Y.; Zhu, Y.; Cao, W.; Baret, F.; Liu, S.; et al. Estimation of Nitrogen Nutrition Status in Winter Wheat from Unmanned Aerial Vehicle Based Multi-Angular Multispectral Imagery. *Front. Plant Sci.* **2019**, *10*, 1601. [CrossRef] [PubMed]
14. Gallegos-Cedillo, V.M.; Diánez, F.; Nájera, C.; Santos, M. Plant Agronomic Features Can Predict Quality and Field Performance: A Bibliometric Analysis. *Agronomy* **2021**, *11*, 2305. [CrossRef]
15. Tshikunde, N.M.; Mashilo, J.; Shimelis, H.; Odindo, A. Agronomic and Physiological Traits, and Associated Quantitative Trait Loci (QTL) Affecting Yield Response in Wheat (*Triticum aestivum* L.): A Review. *Front. Plant Sci.* **2019**, *10*, 1428. [CrossRef]
16. Kakabouki, I.; Beslemes, D.F.; Tigka, E.L.; Folina, A.; Karydogianni, S.; Zisi, C.; Papastylianou, P. Performance of Six Genotypes of Tritordeum Compare to Bread Wheat under East Mediterranean Condition. *Sustainability* **2020**, *12*, 9700. [CrossRef]
17. Olesen, J.E.; Børgesen, C.D.; Elsgaard, L.; Palosuo, T.; Rötter, R.P.; Skjelvåg, A.O.; Peltonen-Sainio, P.; Börjesson, T.; Trnka, M.; Ewert, F.; et al. Changes in Time of Sowing, Flowering and Maturity of Cereals in Europe under Climate Change. *Food Addit. Contam. Part A* **2012**, *29*, 1527–1542. [CrossRef]

18. Cabo, S.; Carvalho, A.; Rocha, L.; Martin, A.; Lima-Brito, J. IRAP, REMAP and ISSR Fingerprinting in Newly Formed Hexaploid Tritordeum (X *Tritordeum* Ascherson et Graebner) and Respective Parental Species. *Plant Mol. Biol. Report.* **2014**, *32*, 761–770. [CrossRef]
19. Martín, A.; Alvarez, J.B.; Martín, L.M.; Barro, F.; Ballesteros, J. The Development of Tritordeum: A Novel Cereal for Food Processing. *J. Cereal Sci.* **1999**, *30*, 85–95. [CrossRef]
20. Villegas, D.; Casadesús, J.; Atienza, S.G.; Martos, V.; Maalouf, F.; Karam, F.; Aranjuelo, I.; Nogués, S. Tritordeum, Wheat and Triticale Yield Components under Multi-Local Mediterranean Drought Conditions. *Field Crops Res.* **2010**, *116*, 68–74. [CrossRef]
21. Visioli, G.; Lauro, M.; Vamerali, T.; Dal Cortivo, C.; Panozzo, A.; Folloni, S.; Piazza, C.; Ranieri, R. A Comparative Study of Organic and Conventional Management on the Rhizosphere Microbiome, Growth and Grain Quality Traits of Tritordeum. *Agronomy* **2020**, *10*, 1717. [CrossRef]
22. Aranjuelo, I.; Cabrera-Bosquet, L.; Araus, J.L.; Nogués, S. Carbon and Nitrogen Partitioning during the Post-anthesis Period Is Conditioned by N Fertilisation and Sink Strength in Three Cereals. *Plant Biol.* **2013**, *15*, 135–143. [CrossRef] [PubMed]
23. Cantarella, H.; Otto, R.; Soares, J.R.; Silva, A.G.D.B. Agronomic Efficiency of NBPT as a Urease Inhibitor: A Review. *J. Adv. Res.* **2018**, *13*, 19–27. [CrossRef]
24. Cantarella, H.; Mattos, D.; Quaggio, J.A.; Rigolin, A.T. Fruit Yield of Valencia Sweet Orange Fertilized with Different N Sources and the Loss of Applied N. *Nutr. Cycl. Agroecosyst.* **2003**, *67*, 215–223. [CrossRef]
25. Dawar, K.; Rahman, U.; Alam, S.S.; Tariq, M.; Khan, A.; Fahad, S.; Datta, R.; Danish, S.; Saud, S.; Noor, M. Nitrification Inhibitor and Plant Growth Regulators Improve Wheat Yield and Nitrogen Use Efficiency. *J. Plant Growth Regul.* **2022**, *41*, 216–226. [CrossRef]
26. Meena, A.K.; Singh, D.K.; Pandey, P.C.; Nanda, G. Dynamics of Dry Matter and Nitrogen Distribution in Transplanted Rice on Mollisols. *J. Plant Nutr.* **2019**, *42*, 749–758. [CrossRef]
27. Silva, A.G.B.; Sequeira, C.H.; Sermarini, R.A.; Otto, R. Urease Inhibitor NBPT on Ammonia Volatilization and Crop Productivity: A Meta-Analysis. *Agron. J.* **2017**, *109*, 1–13. [CrossRef]
28. Cui, M.; Sun, X.; Hu, C.; Di, H.J.; Tan, Q.; Zhao, C. Effective Mitigation of Nitrate Leaching and Nitrous Oxide Emissions in Intensive Vegetable Production Systems Using a Nitrification Inhibitor, Dicyandiamide. *J. Soils Sediments* **2011**, *11*, 722–730. [CrossRef]
29. Soares, J.R.; Souza, B.R.; Mazzetto, A.M.; Galdos, M.V.; Chadwick, D.R.; Campbell, E.E.; Jaiswal, D.; Oliveira, J.C.; Monteiro, L.A.; Vianna, M.S.; et al. Mitigation of Nitrous Oxide Emissions in Grazing Systems through Nitrification Inhibitors: A Meta-Analysis. *Nutr. Cycl. Agroecosyst.* **2023**, *125*, 359–377. [CrossRef]
30. Bouyoucos, G.J. A Recalibration of the Hydrometer Method for Making Mechanical Analysis of Soils. *Agron. J.* **1951**, *43*, 434–438. [CrossRef]
31. Klute, A.; Page, A.L. (Eds.) *Methods of Soil Analysis*, 2nd ed.; American Society of Agronomy, Soil Science Society of America: Madison, WI, USA, 1982; ISBN 978-0-89118-088-3.
32. Nelson, D.W.; Sommers, E. Total Carbon, Organic Carbon, and Organic Matter. In *Methods of Soil Analysis*; Wiley: Hoboken, NJ, USA, 1996.
33. Olsen, S.R. *Estimation of Available Phosphorus in Soils by Extraction with Sodium Bicarbonate*; US Government Printing Office: Washington, DC, USA, 1954.
34. Bremner, J.M. Determination of Nitrogen in Soil by the Kjeldahl Method. *J. Agric. Sci.* **1960**, *55*, 11–33. [CrossRef]
35. Thomas, G.W. Exchangeable Cations. In *Agronomy Monographs*; Page, A.L., Ed.; Wiley: Hoboken, NJ, USA, 1982; Volume 9, pp. 159–165, ISBN 978-0-89118-072-2.
36. Lindsay, W.L.; Norvell, W.A. Development of a DTPA Soil Test for Zinc, Iron, Manganese, and Copper. *Soil Sci. Soc. Am. J.* **1978**, *42*, 421–428. [CrossRef]
37. Mcmaster, G. Growing Degree-Days: One Equation, Two Interpretations. *Agric. For. Meteorol.* **1997**, *87*, 291–300. [CrossRef]
38. Meier, U. *Growth Stages of Mono- and Dicotyledonous Plants: BBCH Monograph*; Open Agrar Repositorium: Berlin, Germany, 2018. [CrossRef]
39. Nelson, D.W.; Sommers, L.E. Total Nitrogen Analysis of Soil and Plant Tissues. *J. AOAC Int.* **1980**, *63*, 770–778. [CrossRef]
40. Shewry, P.R.; Brouns, F.; Dunn, J.; Hood, J.; Burridge, A.J.; America, A.H.P.; Gilissen, L.; Proos-Huijsmans, Z.A.M.; Van Straaten, J.P.; Jonkers, D.; et al. Comparative Compositions of Grain of Tritordeum, Durum Wheat and Bread Wheat Grown in Multi-Environment Trials. *Food Chem.* **2023**, *423*, 136312. [CrossRef] [PubMed]
41. Rouse, W.; Haas, R.H. *Monitoring Vegetation Systems in the Great Plains with Erts*; NASA: Washington, DC, USA, 1974.
42. Gitelson, A.A.; Viña, A.; Ciganda, V.; Rundquist, D.C.; Arkebauer, T.J. Remote Estimation of Canopy Chlorophyll Content in Crops. *Geophys. Res. Lett.* **2005**, *32*, 2005GL022688. [CrossRef]
43. Bailey, S.J. *Using Growing Degree Days to Predict Plant Stages*; MSU Extension Service: Bozeman, MT, USA, 2001.
44. Litke, L.; Gaile, Z.; Ruža, A. Effect of Nitrogen Fertilization on Winter Wheat Yield and Yield Quality. *Agron. Res.* **2018**, *16*, 500–509. [CrossRef]

45. Arduini, I.; Masoni, A.; Ercoli, L.; Mariotti, M. Grain Yield, and Dry Matter and Nitrogen Accumulation and Remobilization in Durum Wheat as Affected by Variety and Seeding Rate. *Eur. J. Agron.* **2006**, *25*, 309–318. [CrossRef]
46. Ciampitti, I.A.; Vyn, T.J. Grain Nitrogen Source Changes over Time in Maize: A Review. *Crop Sci.* **2013**, *53*, 366–377. [CrossRef]
47. Lan, T.; He, X.; Wang, Q.; Deng, O.; Zhou, W.; Luo, L.; Chen, G.; Zeng, J.; Yuan, S.; Zeng, M.; et al. Synergistic Effects of Biological Nitrification Inhibitor, Urease Inhibitor, and Biochar on NH3 Volatilization, N Leaching, and Nitrogen Use Efficiency in a Calcareous Soil–Wheat System. *Appl. Soil Ecol.* **2022**, *174*, 104412. [CrossRef]
48. Meng, Y.; Wang, J.J.; Wei, Z.; Dodla, S.K.; Fultz, L.M.; Gaston, L.A.; Xiao, R.; Park, J.; Scaglia, G. Nitrification Inhibitors Reduce Nitrogen Losses and Improve Soil Health in a Subtropical Pastureland. *Geoderma* **2021**, *388*, 114947. [CrossRef]
49. Guzman-Bustamante, I.; Schulz, R.; Müller, T.; Ruser, R. Split N Application and DMP Based Nitrification Inhibitors Mitigate N_2O Losses in a Soil Cropped with Winter Wheat. *Nutr. Cycl. Agroecosystems* **2022**, *123*, 119–135. [CrossRef]
50. Olšovská, K.; Rybarova, Z.; Sytar, O. Effectiveness of N Fertilizers with Nitrification Inhibitors on Winter Barley Nutrition and Yield. *Sustainability* **2025**, *17*, 2610. [CrossRef]
51. Rawal, N.; Pande, K.R.; Shrestha, R.; Vista, S.P. Nutrient Use Efficiency (NUE) of Wheat (*Triticum aestivum* L.) as Affected by NPK Fertilization. *PLoS ONE* **2022**, *17*, e0262771. [CrossRef]
52. Magney, T.S.; Eitel, J.U.H.; Huggins, D.R.; Vierling, L.A. Proximal NDVI Derived Phenology Improves In-Season Predictions of Wheat Quantity and Quality. *Agric. For. Meteorol.* **2016**, *217*, 46–60. [CrossRef]
53. Zhao, X.; Wang, S.; Wen, T.; Xu, J.; Huang, B.; Yan, S.; Gao, G.; Zhao, Y.; Li, H.; Qiao, J.; et al. On Correlation between Canopy Vegetation and Growth Indexes of Maize Varieties with Different Nitrogen Efficiencies. *Open Life Sci.* **2023**, *18*, 20220566. [CrossRef] [PubMed]
54. Haboudane, D.; Miller, J.R.; Tremblay, N.; Zarco-Tejada, P.J.; Dextraze, L. Integrated Narrow-Band Vegetation Indices for Prediction of Crop Chlorophyll Content for Application to Precision Agriculture. *Remote Sens. Environ.* **2002**, *81*, 416–426. [CrossRef]
55. Sharifi, A. Remotely Sensed Vegetation Indices for Crop Nutrition Mapping. *J. Sci. Food Agric.* **2020**, *100*, 5191–5196. [CrossRef]
56. Hao, T.; Zhu, Q.; Zeng, M.; Shen, J.; Shi, X.; Liu, X.; Zhang, F.; De Vries, W. Impacts of Nitrogen Fertilizer Type and Application Rate on Soil Acidification Rate under a Wheat-Maize Double Cropping System. *J. Environ. Manag.* **2020**, *270*, 110888. [CrossRef]